JOURNAL OF PROPULSION AND POWER
Vol. 21, No. 1, January–February 2005

Plasma Ignition and Combustion of JA2 Propellant

Jianquan Li,* Thomas A. Litzinger,† and Stefan T. Thynell†
Pennsylvania State University, University Park, Pennsylvania 16802

Experiments were performed to investigate the effects of various parameters on plasma-driven ignition and combustion of a double-base propellant under closed-chamber conditions. The parameters varied include input electrical energy, nozzle length and inner diameter, nozzle exit to propellant distance, as well as propellant sample thickness. Chamber pressure was measured to determine the ignition delay and to deduce the regression rate. High-speed images of the plasma jets and combustion event were also recorded. At low plasma energies, rapid, plasma-driven burning occurred, but self-sustained burning was not achieved. With moderate plasma energies, combustion of the propellant exhibited a two-stage burning behavior: one stage of plasma-driven rapid burning that occurred during the plasma pulse and a second stage of slower self-sustained burning that occurred with a clear delay after the first stage. When plasma energy was increased further, the two-stage behavior became less distinct and eventually disappeared, leaving only one stage of burning. Nozzle length and diameter affected the ignition and combustion characteristics as a result of energy losses from the plasma as it flows through the nozzle. The propellant burning behavior is also affected by both nozzle–sample distance and sample thickness. High-speed images revealed vigorous motion of gases in the closed chamber, which was induced by the plasma jet. Also, the images showed what appeared to be JA2 fragments; this observation was confirmed by recovery of fragmented propellant after some of the tests.

Nomenclature

c	=	specific heat
d_c	=	capillary diameter
d_N	=	nozzle inner diameter
E	=	electrical energy stored in plasma generator
E_{vap}	=	energy for vaporization at standard state
h_{vap}	=	heat of vaporization at normal boiling point
I_1	=	electrical current flowing through capillary plasma
I_2	=	electrical current flowing parallel to I_1
L_N	=	length of nozzle (cathode)
$L_{\text{c–s}}$	=	distance between capillary exit to propellant sample
$L_{\text{n–p}}$	=	distance between nozzle exit to stagnation plate
$L_{\text{n–s}}$	=	distance between nozzle exit to propellant sample
m_s	=	mass of JA2 propellant sample
p	=	pressure
R	=	electrical resistance
t	=	time
t_s	=	thickness of propellant sample
V_c	=	volume of test chamber
Δp	=	peak pressure rise caused by propellant combustion only
$\Delta\tau$	=	time duration of the second stage of burning

Introduction

THE electrothermal–chemical (ETC) propulsion concept has been the subject of substantial research activities as reviewed in Refs. 1–7. This propulsion concept, which utilizes electrically generated plasma for ignition, has potential application in both medium- and large-caliber weapon systems. Results from laboratory experiments and actual firing tests have revealed that the use of ETC plasma ignition can offer several attractive benefits over conventional chemical powder ignition, such as precision ignition in terms of shorter and more reproducible ignition delay,[8] mitigation of gun performance sensitivity to ambient temperature,[9,10] better controlled propellant mass generation rates,[11] and the ability to ignite reliably low-vulnerability ammunition propellants[12] and high loading density propellant charges.[13,14] However, optimization of the ETC igniter design relies on a clear and complete understanding of the underlying fundamentals that account for these observed benefits.

The ignition source of ETC guns is in the form of an electrothermal plasma that is produced through a rapid capacitive discharge process, where electrical energy is converted into various other forms, including internal, kinetic, and chemical energies. The submillisecond duration of the electrical discharge is achieved through selection of the electrical circuit components, generally consisting of the capacitors, the inductors, and the plasma (the resistor[15]) generated by exploding a thin metallic wire in a capillary and sustained by the ablation of surrounding capillary wall material of either the propellant[16] or a hydrocarbon polymer.[17–21] The electrical connection between the electrodes that is initially provided by the wire is then continued by the plasma. Using the trigger wire in the capillary allows a highly efficient initiation and establishment of the plasma.[22] The behavior of the electrical circuit, the trigger wire explosion phenomenon, as well as the fluid mechanics of the plasma propagation into a stagnant atmosphere are fairly well understood.[23–29] However, many other aspects are much less understood, such as the underlying causes for the measured shorter ignition delay, enhanced burn rate during the electrical discharge, and differences in the extent of the interaction between the plasma and various propellants.

Numerous studies have been conducted to provide basic or phenomenological information about the plasma–propellant interaction process. Early studies revealed the ability to minimize the effect of the propellant's initial temperature on the burn rate.[30] This was accomplished by adjusting the plasma injection process and power levels, to achieve breech pressures at their maximum levels for a broad range of initial temperatures.

Several works have been performed trying to characterize the ETC plasma impact on the ignition and combustion of JA2 propellant during and following the plasma pulse. Koleczko et al.[16] have studied burn-rate differences between graphite-containing and graphite-free JA2. The burn-rate enhancement for transparent JA2 was significant and lasted well beyond the duration of the plasma pulse. For graphite-containing JA2, burn-rate enhancement was much less, but much larger compared to the use of a conventional igniter. The results were explained by 1) in-depth absorption of radiant energy that

Received 17 October 2003; revision received 7 April 2004; accepted for publication 29 April 2004.

*Research Assistant, Department of Mechanical and Nuclear Engineering. Student Member AIAA.

†Professor, Department of Mechanical and Nuclear Engineering. Senior Member AIAA.

produced decomposition of energetic molecules, 2) formation of internal voids (porous structure) and fragmentation of propellant by decomposition gases, and 3) increased surface area for conversion of propellant into final products. Birk et al.[17] studied JA2 response to plasma in both interrupted and noninterrupted test configurations and found burn rate of JA2 was enhanced by 40–120% during the plasma pulse but not after it. Pesce-Rodriguez et al.[31] and Beyer and Pesce-Rodriguez[32] used desorption-gas chromatography–mass spectroscopy on recovered JA2 samples from interrupted tests. They concluded that subsurface reactions occurred in plasma-exposed samples based on the evidence of in-depth (0.75 mm) denitration of JA2 possibly due to radiation absorption, although in-depth profile was not consistent with radiation absorption by Beer's law. No conclusions were made whether denitration was caused by thermal or photochemical effects. In addition, microscopic investigations revealed the formation of pits and wormholes that produced an increased surface area and possible burn-rate augmentation. Katulka et al.[33] used a configuration where the propellant samples were either fully exposed to plasma normal impingement, or covered with Mylar® or aluminum films to separate conductive and convection effects from plasma radiation effect. The Mylar film is opaque for wavelengths below 300 nm. In general, Mylar-covered samples showed little or no evidence to the effects of radiation, because ignition did not occur. Hence, the UV radiation component appears to be important. Bourham et al.[34] studied the effects of plasma impinging angle on the ignition and combustion characteristics of JA2. Results showed evidence of an enhanced burn rate at pressures of 55–90 MPa over 400-μs pulse length, and 20–40% enhancement in burn rate was achieved for parallel injection, whereas a factor of three increases in burn rate was observed with normal injection. Taylor[35] reported that results from small-scale closed vessel tests and large-caliber 155 mm tests suggested radiative energy transfer from plasma to propellant is negligible for ignition, but metallic vapor deposition is important to efficient ignition and with a shorter ignition delay. Also, in Taylor's work,[36] it was found that wire mass, capillary dimensions, and propellant composition and initial temperature made no measurable difference in the ignition delay. However, the amount of electrical discharge energy had a distinctive influence on ignition delay.

These research efforts have provided many insights to the various mechanisms and, hence, a greatly improved understanding of plasma ignition mechanisms. However, a complete understanding is critical to the development of the ETC technology; therefore, continuing research is needed. This paper reports results from recent experimental work on characterizing the ignition and combustion of a double-base propellant, JA2, driven by the ETC capillary plasma. An effort of visualizing the plasma–propellant interaction during ignition and combustion was made, which is believed to be very helpful to aid in the interpretation of many other experimental data. The overall objective of this work is to gain insights from parametric studies that will contribute to the formulation of a complete understanding of the various chemical and physical processes occurring in plasma–propellant interactions.

Experimental Apparatus and Approach

Plasma Generator

The capillary plasma-generation system is schematically shown in Fig. 1. The pulse-forming network (PFN) is based on a resistance–inductance–capacitor circuit, which is mainly composed of an energy storage component that consists of two high-voltage fast-discharge capacitors connected in parallel to yield a total capacitance of 192 μF, pulse-shaping components including a 20-μH inductor and a crowbar diode, and a floating high-voltage mercury switch (ignitron) as the trigger unit. The capacitors can be charged up to 10 kV, yielding maximum energy storage of 9.6 kJ. The plasma chamber consists of a capillary liner, a fine metallic wire, electrodes, and other conducting or nonconducting housing hardware. The capillary liner is typically made of either high-density polyethylene (PE, $[C_2H_4]_n$) or polycarbonate (Lexan, $[C_{16}H_{14}O_3]_n$), which is machined to have a bore length of 26 mm and a typical diameter of 3.2 mm. Located at either end of the capillary are two electrodes made of erosion-resistant material, elkonite, a copper–tungsten alloy (30% Cu, 70% W). Inside the capillary is a fine copper filament that is connected between the electrodes and serves as the discharge initiator. After being formed immediately on triggering of the ignitron, the plasma flows through a nozzle that has typical dimensions of 3.2 mm (inner diameter) and 26 mm (length) into open air or a closed chamber.

Test Chambers

Two closed chambers with different configurations were used in the experiments. The first one, as shown in Fig. 1, has dimensions of 3.5 cm in length and 2.1 cm in diameter, corresponding to a net volume of 15.8 cm^3. An insert was used to allow variation in the chamber volume, and for tests conducted with this chamber, the actual volume was 6.5 cm^3.

The second one is an optically accessible windowed chamber (shown in Fig. 2), which was fabricated to allow photography of propellant ignition and combustion processes. The windowed chamber measures 3.5 cm long with a 4.3 cm diameter, yielding a net volume about 48 cm^3. The chamber is equipped with a 2.0-cm circular viewing port, and the optical window can withstand pressures up to 20 MPa.

In general, a sample holder, with one end screwed into the end plate of the closed chamber, brings the propellant sample close to the nozzle exit to enable normal exposure to the plasma jet. For tests with no propellant, an inert substitute having the same size with the propellant sample was used to maintain the same chamber volume. Two pressure transducers (P.T.) were mounted in different locations

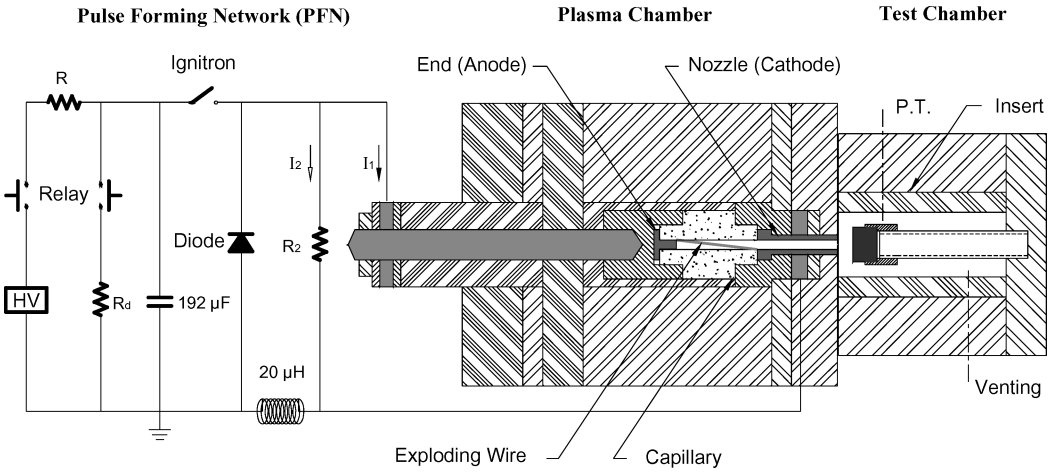

Fig. 1 Schematic of test setup for plasma ignition.

Table 1 Effect of plasma energy on discharge and burning behavior of JA2 with $m_s = 500$ mg and $V_c = 6.5$ cm^3

E, kJ	I_{1_peak}, kA	$\tau_{\text{pulse-length}}$, μs	$p_{\text{plasma-peak}}$, MPa	$p_{\text{peak-in-pulse}}$, MPa	Δp,[a] MPa	$\tau_{\text{second-stage}}$, ms	$\tau_{\text{end-combustion}}$, ms	$\Delta\tau$,[b] ms
0.38	3.15	179	4.8	5.4	0.6	143	191	48
0.60	4.76	180	7.1	8.5	1.4	6.5	49	43
0.86	6.32	191	11.0	12.4	1.4	2.2	33	31
1.56	9.38	262	16.1	23.0	6.9	0.39	7.9	7.5
2.40	12.70	310	21.3	42.1	20.8	0.31	1.38	1.1

[a] $\Delta p = p_{\text{peak-in-pulse}} - p_{\text{plasma-peak}}$. [b] $\Delta\tau = \tau_{\text{end-combustion}} - \tau_{\text{second-stage}}$.

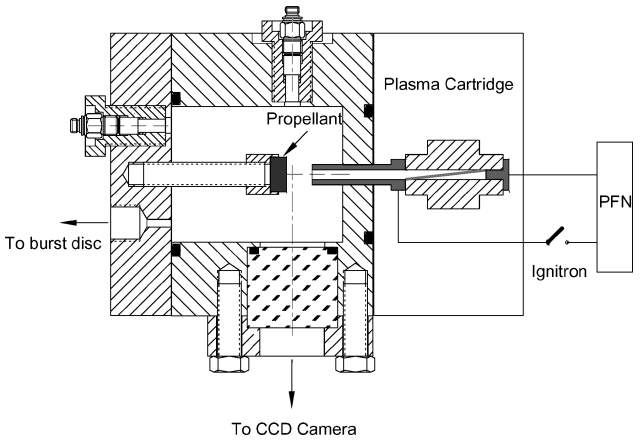

Fig. 2 Sectional view of the windowed chamber.

to allow simultaneous measurement of pressure time history in the chamber. A venting hole was connected to a solenoid valve for depressurization of the chamber as needed.

Diagnostics

Diagnostics included measurements of electrical currents and chamber pressures resulting from plasma jet expansion and propellant combustion and capture of images of evolving plasma jets and burning propellant. Pearson coils were used to measure the currents including I_1, which flows through plasma inside the capillary, and I_2, which flows parallel with I_1 but though a non-inductive resistor bank (denoted as R_2 in Fig. 1). The instantaneous voltage across the plasma can then be deduced from I_2 and the resistance of R_2, which is connected in parallel with the flow of I_1.

Two types of Kistler pressure transducers were used, with Model 211B3 having a measuring range of 0–500 psig (0–3.45 MPa) and a rise time of 2 μs for lower pressure measurement and Model 211B1 of a much higher measuring range of 0–10,000 psig (0–68.95 MPa) and a rise time of 1 μs for higher chamber pressure measurement. To minimize thermal and electromagnetic effects of plasma on the pressure transducers in closed-chamber testing, recess mounting was adopted to allow the use of a thin layer ($\sim$1 mm) of vacuum grease between the sensor diaphragm and plasma. This treatment proved to be effective in protecting the pressure transducers from overheating and from direct exposure to the charged particles in the plasma. A check with compressed air showed no evidence that this grease layer affected the rise time of the pressure transducer.

Images were taken using an intensified, multiple charge-coupled device (CCD) imaging system, Cordin 222-B, which consists of 8 CCDs and is capable of acquiring 16 images, each with a pixel resolution of 1300 by 1030, a 10-bit dynamic range, and exposure gates down to 10 ns. The first eight images can be acquired at a framing speed of up to 10^8 frames/s, followed by a delay of 1 μs, and then a second set of eight images at the same framing rate is acquired.

A Nicolet 120 MultiPro high-speed data acquisition system along with its ProView software was used for pressure and current measurements.

Results and Discussion

Results from pressure measurements under various test conditions will be presented first, followed by discussion of the photographic results of the plasma jets and the burning propellant. The propellant used in all tests was a double-base gun propellant JA2. The test samples were cut from JA2 cylindrical sticks, which have a diameter of 10.9 mm and seven 0.5-mm perforations.

Pressure Measurements

Two sets of experiments were performed to investigate the effects of plasma parameters and test conditions on ignition and combustion characteristics of JA2. The first set of tests was conducted in the smaller chamber (6.5 cm^3) to achieve a higher propellant loading density. During the tests, the input electrical energy was varied from 0.38 to 2.40 kJ. The second set of tests was conducted to investigate the effects of nozzle length and inner diameter, the distance from nozzle exit to propellant sample (hereinafter referred to as nozzle–sample distance) $L_{\text{n–s}}$, and propellant sample thickness t_s. These experiments were performed in the 48-cm^3 windowed chamber to allow imaging as well as pressure measurements to be carried out. Both PE and Lexan capillaries of 3.2 mm diameter were used in these tests; however, the type of capillary material did not result in any observable differences in ignition or combustion of the propellant.

Plasma Energy Effect

It is expected that more electrical energy input to the plasma will ensure more effective ignition of the propellant charge. In actual ETC weapon system applications, however, minimizing the requirement of input electrical energy for ignition is important for overall system design. Therefore, tests were conducted to determine the minimum electrical energy needed to ignite the propellant charge effectively and reliably. Typical results of tests with differing input electrical energies are summarized in Table 1 and plotted in Figs. 3–6. Each test used the same amount of JA2, approximately 500 mg, to give a loading density about 0.08 g/cm^3, and the nozzle–sample distance was held at 5 mm for all tests.

In Table 1, E refers to electrical energy stored in the pulsed power source; typically about 95% of the stored energy is deposited into the generated plasma through ohmic heating. The duration of discharge pulse, $\tau_{\text{pulse-length}}$, is measured from time zero to the time when the discharge current has decreased to a value on the order of 10^{-3} kA. Here $p_{\text{plasma-peak}}$ is the peak pressure caused by the plasma jet alone, with no propellant present; it was obtained by firing the plasma into the chamber with an inert substitute in place of the propellant sample. The pressure rise, Δp, is the difference between $p_{\text{plasma-peak}}$ and $p_{\text{peak-in-pulse}}$; the latter is the in-pulse peak pressure resulting from a combined effect of plasma jet expansion and propellant combustion during the plasma pulse. The start of the second stage, $\tau_{\text{second-stage}}$, is defined as the time when pressure starts to rise for a second time after the pulse. The time for completion of burning, $\tau_{\text{end-combustion}}$, is taken as when pressure trace reaches a second peak.

Figure 3 presents the chamber pressure as a function of time on different timescales, 0–5 and 0–300 ms; the shorter timescale shows details of the plasma-driven burning. Figure 4 presents a comparison of discharge power for five plasma energy levels, which illustrates variation in peak power and pulse length. Figure 5 shows variations in pressure rise due to hot gaseous products from ablation and/or burning of JA2 samples during the pulse.

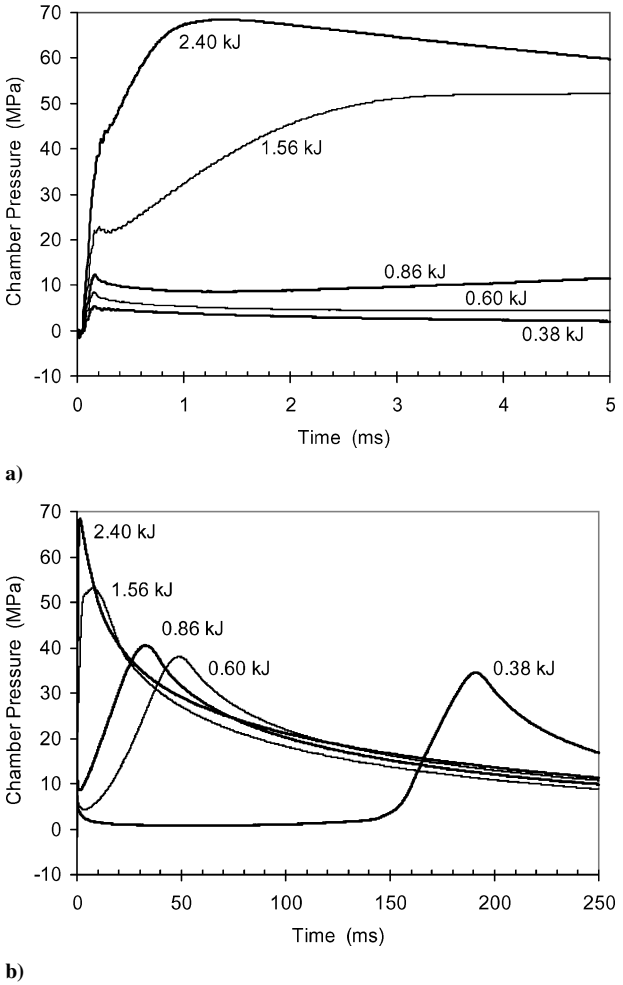

Fig. 3 Effect of plasma energy on ignition and combustion of JA2: $V_c = 6.5$ cm^3, $m_s = 500$ mg, and $L_{n-s} = 5$ mm.

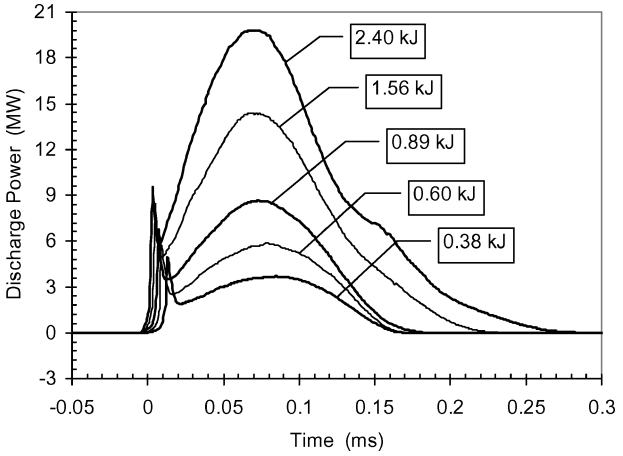

Fig. 4 Discharge power at varied electrical energies.

As expected based on work of past researchers,[30] input energy has a significant influence on the ignition and entire burning of the propellant. With the energy at 1.56 kJ, the pressure trace in Fig. 3a clearly indicates a two-stage burning behavior: a fast combustion within the plasma pulse that appears to extinguish before the pulse ends at about 0.26 ms, which is followed by a second ignition after which the propellant sample burns to completion over a relatively long period of time (7.5 ms). When plasma energy is increased (2.40 kJ data), the two-stage behavior becomes much less distinct; burning is sustained from plasma-driven ignition to completion and occurs over a much shorter period of time about 1.1 ms. When less

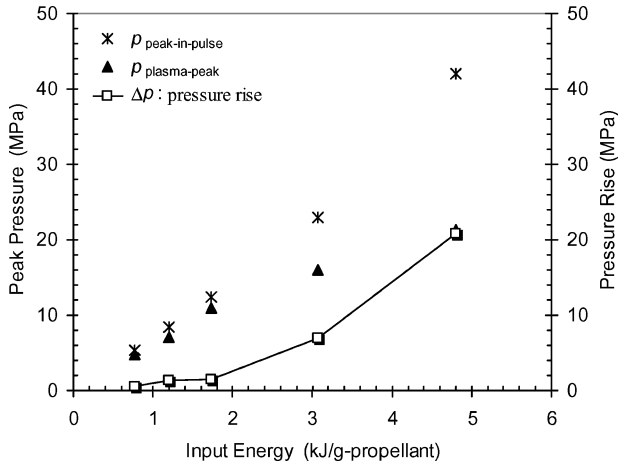

Fig. 5 Plasma energy effect on peak pressures and in-pulse pressure rise.

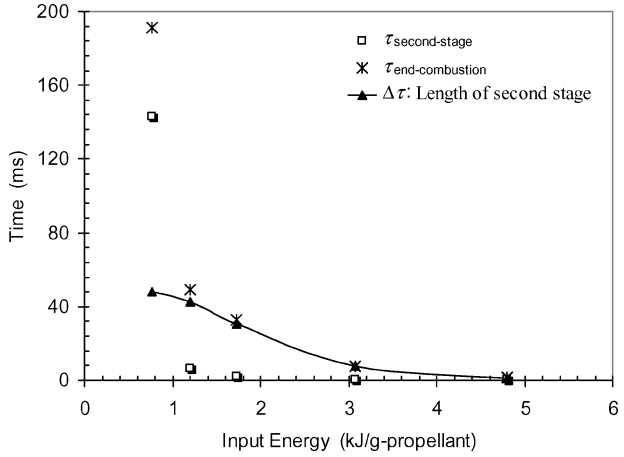

Fig. 6 Plasma energy effect on the second stage of burning.

plasma energy is used, the pressure rise due to burning during the plasma pulse decreases (Fig. 5), and the delay time between the two stages lengthens. Figure 6 presents a summary of the timescales of the second-stage burning as a function of input energy. The delay time and length of the second stage vary strongly with input energy.

These results indicate that the minimum electrical energy required to achieve sustained burning without significant two-stage burning behavior is approximately 1.56 kJ for a loading density of 0.08 kg/cm^3 under the current test conditions. With this input energy, however, other changes in test conditions can still bring about significant changes in JA2 burning behavior, as will be discussed in the following sections.

Nozzle Geometry Effect

As the plasma flows through the nozzle (cathode), it experiences viscous effects and heat transfer. It is, therefore, likely that nozzle dimensions would affect the plasma flow and the actual energy available to ignite the propellant. Therefore, tests were conducted to determine the effects of the nozzle length and inner diameter on the plasma and its interaction with JA2.

Although the ETC plasma is sustained by ablation of capillary wall material, for a plasma generator having a configuration shown in Fig. 1, the total mass in the plasma jet comprises contributions from several sources, including the end electrode (anode), the trigger wire, the nozzle (cathode), the capillary, and the air that is initially in the capillary. Generally, because the nozzle undergoes intense radiative and convective heating by the hot plasma flowing through it at high velocities, ablation of the nozzle surface material provides a major fraction to the total plasma mass. As a result, the mass of metallic particles dominates the total mass of the plasma jet.

Table 2 Effect of nozzle dimensions on plasma mass: $E = 1.56$ kJ, $d_N = 3.2$ mm, Lexan

Test	Nozzle i.d., mm	Nozzle length, mm	Plasma mass sources					Total mass, mg
			Capillary, mg	Nozzle, mg	End (anode), mg	Wire, mg	Air,[a] mg	
0291	4.7	13	5.1	1.6	1.4	2.7	0.2	11.0
0293	3.2	13	6.5	5.1	1.6	2.7	0.2	16.1
0295	3.2	28	6.1	14.8	1.6	2.7	0.2	25.4

[a]Air initially trapped in the capillary.

Table 3 Properties of electrode material[a]

Material	g/mol	c kJ/kg/K	MP, K	BP, K	h_{vap}, kJ/mol	E_{vap}, kJ/g
Cu	63.546	0.38	1356.6	2843	300.3	5.69
W	183.85	0.13	3683.2	5773	824.0	5.19

[a]Copper and tungsten.

Table 4 Plasma energy loss due to nozzle ablation, $E = 1.56$ kJ

Test	Nozzle i.d., mm	Nozzle length, mm	Ablation of nozzle, mg	Energy for ablation, kJ	Fraction of E, %
0291	4.7	13	1.6	0.009	0.58
0293	3.2	13	5.1	0.027	1.84
0295	3.2	28	14.8	0.079	5.33

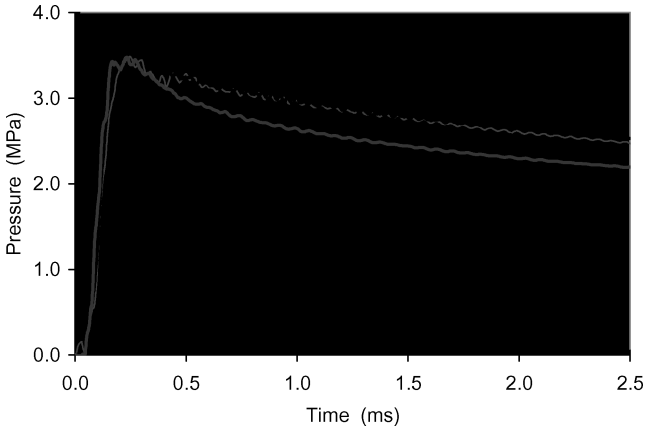

Fig. 7 Effect of nozzle dimensions on plasma chamber pressure: $V_c = 48$ cm^3 and $E = 1.56$ kJ.

However, in terms of mole fraction, it is the species ablated from the hydrocarbon capillary that have dominance (about 90%) over all other species.[37]

Table 2 lists typical results that compare the influence of nozzle length and inner diameter on the contributions of each source to the total mass. Distinctive differences in nozzle ablation mass were found for the three nozzles. The energy loss due to ablation of the Cu/W alloy used in the nozzle was estimated under the assumption that ablation was caused by vaporization only, which is reasonable given the high plasma temperature [>10,000 K (Ref. 19)] well above the boiling points of copper and tungsten. The data used in this calculation, including molecular weight (MW), melting point (MP) and boiling point (BP), are presented in Table 3.

Table 4 summarizes the energy loss associated with ablation and shows that it accounts for as much as 5.33% for the longer nozzle, but only 0.58% for the shorter nozzle of a 3.2 mm i.d. This difference is large enough that it should lead to differences in plasma behavior. Figure 7 presents the results of chamber pressure when plasma entered the closed chamber through these nozzles. As expected, the discrepancies in pressure traces are correlated reasonably well to those found in ablation energy losses.

Not surprisingly, the use of these nozzles would produce difference in the ignition of JA2 by the plasma. Representative results of using these nozzles are presented in Figs. 8 and 9. For illustration purposes, also included in Fig. 8 are the variations in nozzle

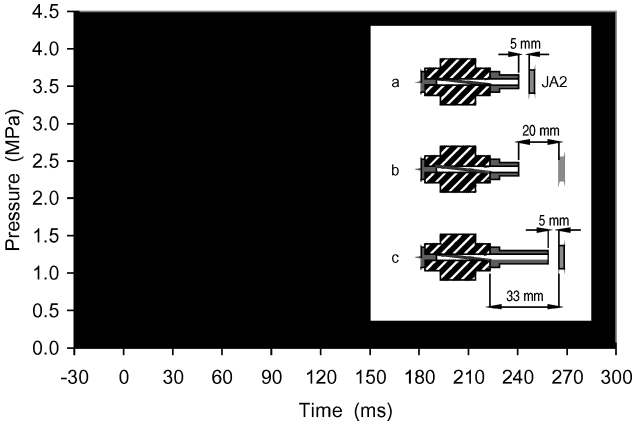

Fig. 8 Nozzle length effect on JA2 burning behavior: $V_c = 48$ cm^3, $E = 1.56$ kJ, $m_s = 255$ mg, and $d_N = 3.2$ mm.

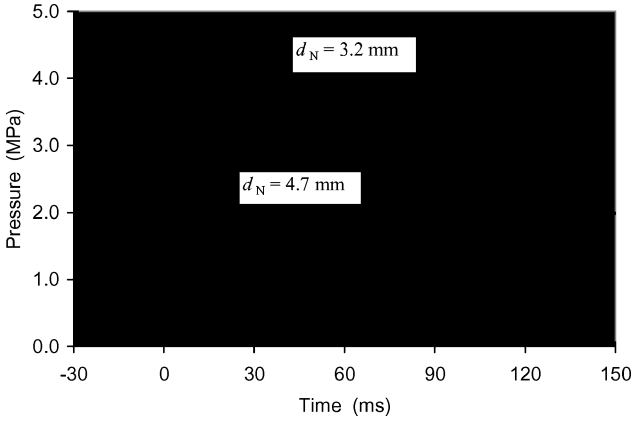

a)

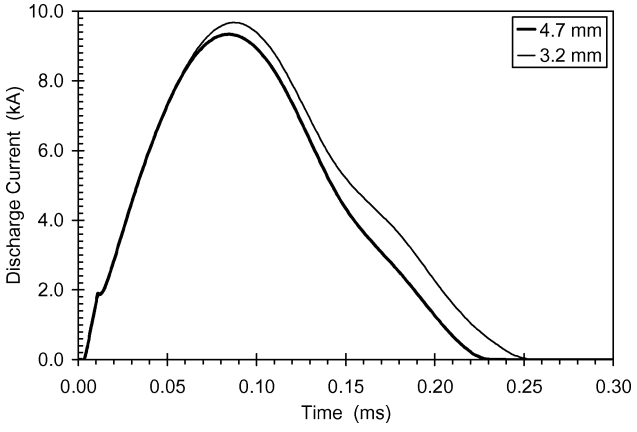

b)

Fig. 9 Nozzle i.d. effect on JA2 burning behavior and discharge current: $E = 1.56$ kJ, $m_s = 255$ mg, $L_N = 13.5$ mm, and $L_{n-s} = 5$ mm.

configuration corresponding to the plots labeled as a, b, and c. Three comparisons can be made based on the results in Fig. 8: a vs b, a vs c, and b vs c. Comparison of a and b illustrates the effect of the nozzle–sample distance, which will be discussed in detail later; thus, discussion here will be focused on the last two cases. As indicated, the nozzle–sample distances in a and c were kept at 5 mm, but test c used a longer nozzle (28 mm), resulting in a longer ignition delay and a slower burn rate and, hence, a lower peak pressure due to greater energy loss to the chamber walls during combustion. It appears that the longer nozzle caused more energy loss from the plasma, resulting in longer ignition delay times. Another possible reason is that although the nozzle–sample distances were the same, the distances from the capillary exit to the sample, L_{c-s}, were different, so that, with the longer nozzle, the plasma has to travel a longer path to reach the propellant. In addition to enabling more heat transfer from the plasma to the nozzle wall, the longer nozzle also enables more momentum loss due to the viscous boundary layer that develops along the nozzle inner surface, which then reduces the mass flow rate of the plasma at the nozzle exit, resulting in a reduction in the heating rate of the propellant by the plasma. This boundary-layer effect may be further evidenced to some extent by comparing test c with b, where the propellant sample was kept at the same location relative to the capillary exit, but a shorter nozzle was used to reduce both nozzle ablation effect and boundary-layer effect. The resultant difference in pressure traces can be seen but is much less pronounced compared to that of a vs c, which may suggest that L_{c-s} is more critical than L_{n-s} to propellant ignition.

However, it seems that the differing behaviors in JA2 ignition and burning cannot be explained only by those effects already mentioned, as shown in Fig. 9a, which presents typical results from tests that used nozzles of the same length (13 mm) but different i.d. As shown in Tables 2 and 4, the ablation mass and ablation-associated energy loss of the 3.2-mm i.d. nozzle are three times that of the 4.7-mm i.d. nozzle, and based on the foregoing analysis, longer ignition delay and lower burn rate should be seen with the smaller i.d. nozzle, but the result shows the opposite trend. Accordingly, some other factors related to nozzle i.d. must exist that exert a major influence on the ignition process.

In the formation of the capillary plasma, the electrical energy is converted into thermal energy of the plasma through ohmic heating, and thus, the temperature and pressure of the plasma are closely related to the discharge current. Figure 9b shows a comparison of the discharge current when using the two different nozzles. It is likely that the differences in the peak current and the discharge pulse length are responsible for the resultant behaviors in the ignition and combustion of the propellant. This current effect has also been evidenced in the work of Kappen and Beyer,[38] who examined the response of a transparent JA2 to plasma radiation and found that with almost the same energy a higher peak current caused more structural damage of the propellant.

Effect of Nozzle–Sample Distance

Another factor that has an influence on the ignition and combustion of the JA2 propellant is the nozzle–sample distance. It has been found in a previous work that a shorter L_{n-s} enables more ablation of the propellant.[39] In the present work, experiments with different values of L_{n-s} were carried out to study how this parameter would affect the burning behavior of the propellant. A typical result is in Fig. 10. For each test, a JA2 sample of 260 mg (2.3 mm thick) was used, and the electrical energy was kept at 1.56 kJ. Nozzles having the same dimensions ($d_N = 3.2$ mm and $L_N = 26$ mm) were used for these tests, and three nozzle–sample distances were considered, including 3, 8, and 15 mm. Differences can be seen in both early response of the propellant and in its overall burning characteristics. It appears that the response of the JA2 sample to plasma during the pulse is negligible for the test of L_{n-s} at 15 mm because its pressure trace is very similar to that of the test with no propellant. For the two shorter nozzle–sample distances, plasma–propellant interaction was evident within the pulse, an indicator of early conversion of the propellant sample from solid to gaseous products due to ablation and decomposition.

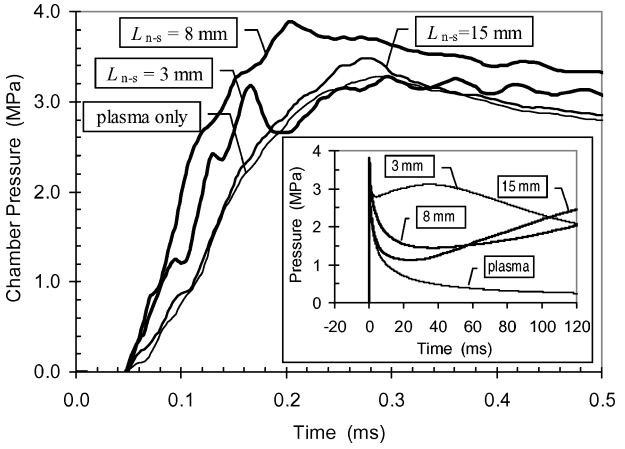

Fig. 10 Influence of nozzle–sample distance on burning behavior of JA2: $m_s = 260$ mg, $V_c = 48$ cm^3, and $E = 1.56$ kJ.

This effect is essentially attributed to the dependence of heat transfer rates on the nozzle–sample distance, which affects the heating of the propellant in several ways. First, as L_{n-s} increases, the plasma mass flux that comes to a contact with the propellant becomes smaller, resulting in a lowered heat transfer rate from the plasma to the propellant. Second, higher values of L_{n-s} cause more reduction in the recovery of temperature due to radiation loss and possibly also because of the formation of stagnation bubbles in the region between the propellant surface and the Mach disk in the plasma jet. The stagnation bubble is formed as a result of interactions of plasma jet shocks with the plate shock that is generated when a freejet is impinging on a plate.[40,41] Consequently, the convective heat transfer rates will slow down with longer L_{n-s}. Third, from a radiation heat transfer point of view, because the solid angle projected on the sample surface from any point in the jet is inversely proportional to the square of the distance from this source point to the sample, radiative heating of the propellant by the plasma will be attenuated with longer L_{n-s}. Fourth, as will be seen in the photographic study, at $L_{n-s} = 5$ mm, the mushroom-shaped bright core, representing the hottest part of the plasma jet, maintains contact with the propellant surface during most of the plasma event. Within this hottest mushroom region, although the local density is much higher than that at $L_{n-s} = 15$ mm, recombination reactions may not prevail yet because the temperature is still extremely high, and therefore, plasma species are present mainly as small ions and radicals, which would actively participate in the chemical reactions that lead to ignition of the propellant.

Effect of Sample Thickness

Heat flux measurement by Williams and White[42] found an effect of sample thickness on the bulk temperature rise of JA2 after exposure to the plasma, which showed that the temperature rise of 1-mm-thick JA2 was twice that of a 2-mm-thick JA2 sample. Hence, it is expected that thinner JA2 samples should ignite easier with shorter ignition delay than thicker ones. Experiments were performed to explore this effect. The results are shown in Fig. 11, where three sample thicknesses were considered including 1.5, 2.8, and 3.2 mm, which correspond to weights of 163, 317, and 360 mg. As shown, a clear correlation can be seen between the sample thickness and the ignition delay. The pressure curves differ from those presented in Fig. 3 due to the use of the large combustion chamber (48 cm^3), which lowered the chamber pressures and thus also the burning rates. Bulk temperature rise may explain the sample thickness effect; however, propellant fragmentation leading to increased burning surface area may also be playing a role. As will be discussed with the following photographic results, the thinner JA2 samples would break into smaller fragments under the severe thermal and gas dynamic conditions induced by the plasma jet.

Photography of Evolving Plasma Jets and Burning JA2

In an earlier work,[39] an attempt was made to photograph the response of a JA2 sample to the plasma in an open-air configuration, and a typical result is shown in Fig. 12. In this test, the sample holder brought the JA2 sample close to the nozzle exit with L_{n-s} at 5 mm. The core of the plasma maintained contact with the sample surface throughout the plasma discharge, but no self-sustained burning was achieved due to the lack of confinement of the plasma–propellant interaction. Although the 4.5-mm-thick JA2 sample survived the normal impingement of the plasma jet, plasma interaction caused a 25-mg mass loss of the propellant. The images (Fig. 12) did not show observable evidence of ignition of this part of propellant, which is likely attributed to a luminosity overlapping effect.

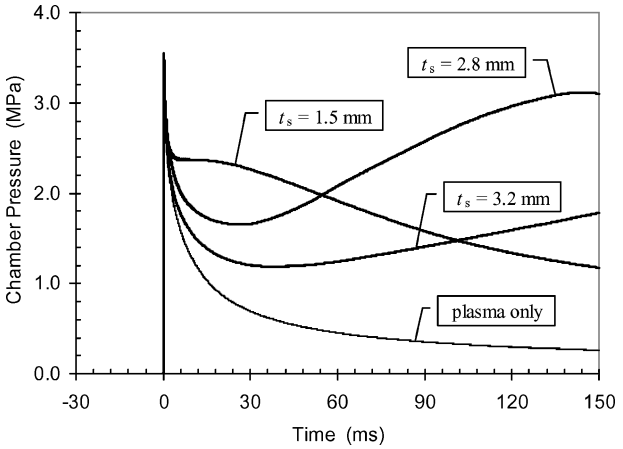

Fig. 11 Effect of sample thickness on burning behavior of JA2: V_c = 48 cm^3, E = 1.56 kJ, and L_{n-s} = 5 mm.

The present photographic study continued the previous work but was conducted in a closed chamber in an attempt to achieve ignition. Initial tests were conducted in hope to capture plasma ignition of JA2 samples within the discharge pulse by taking advantage of the high temporal resolution of the CCD imaging array. However, it was found that the luminosity of burning JA2 was much less than that of the plasma, and so no images were obtained. In principle, appropriate filters can optically attenuate the plasma brightness but may not ensure a solution to solve this problem. Alternatively, the brightness of plasma can be separated from that of burning JA2 by prolonging the delay between the first stage and second stage of burning through the use of lower plasma energy, larger L_{n-s} values, or larger chamber volume. In addition, to maximize the viewing area of the optical window, and to have a relatively low operating pressure to protect the window, a larger chamber volume is more desirable. Therefore, the windowed chamber was designed to have a relative large volume (48 cm^3) for the photographic work.

It has been found that, when using a PE capillary, a considerable amount of soot was formed when the plasma cools after entering the chamber. Compared to PE, Lexan produces less soot due to the presence of oxygen in its composition. Therefore, Lexan capillaries were used to minimize soot contamination of the chamber window.

Figure 13 presents a comparison of evolving plasma images in the closed chamber to that in open air, with test setups and image

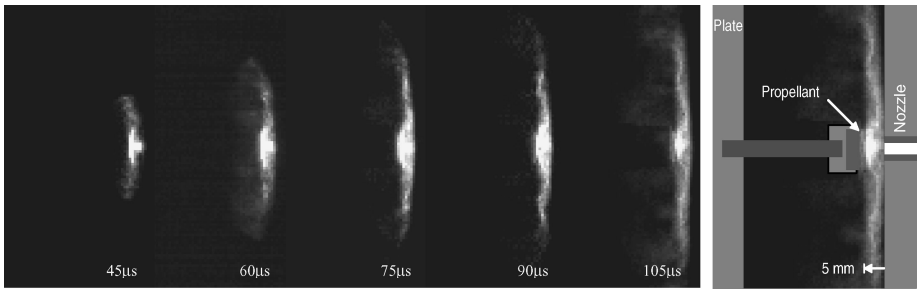

Fig. 12 Typical 1.56-kJ plasma jet impinging on JA2 propellant sample in open air at nozzle–sample distance of 5 mm.

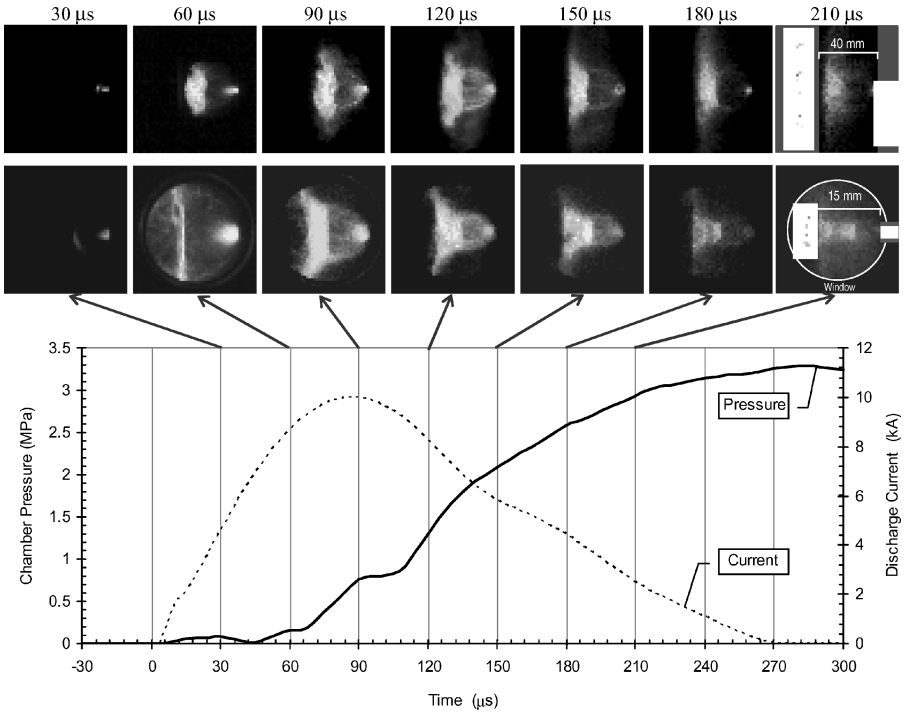

Fig. 13 Evolving plasma jets (E = 1.56 kJ) in open-air (top) and closed-chamber (bottom) and discharge current and plasma pressure in the chamber.

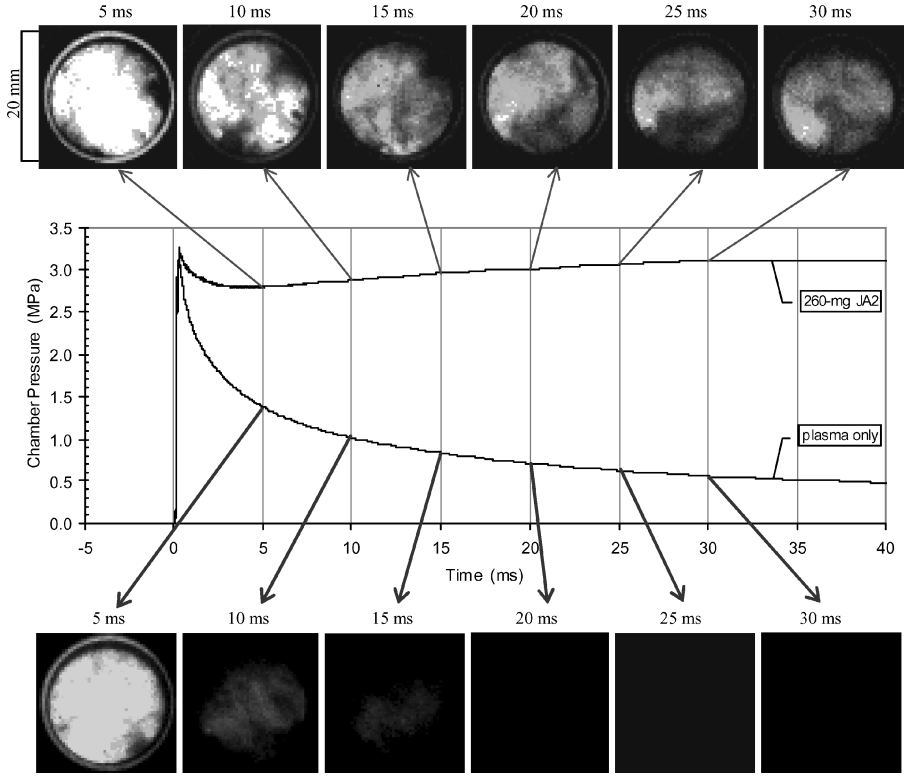

Fig. 14 Plasma-ignition burning JA2 in a closed chamber, $V_c = 48$ cm^3, $E = 1.56$ kJ, and $L_{n-s} = 5$ mm (top); plasma-induced hot gases under the same test conditions (bottom); and corresponding pressure traces from tests with and without JA2 (center).

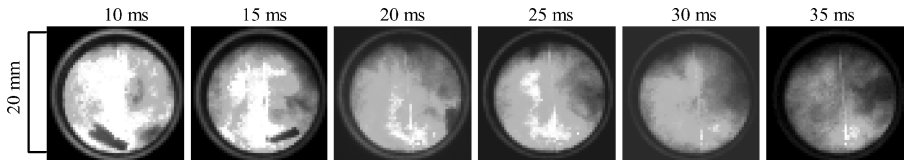

Fig. 15 Plasma-ignition burning JA2 (1.8 mm thick, 200 mg) in closed chamber showing a fragmented piece: $V_c = 48$ cm^3, $E = 1.56$ kJ, and $L_{n-s} = 5$ mm.

sizes shown in the last image of each row. A discharge current trace representative for both closed-chamber and open-air configurations is presented to illustrate the pulse duration and the correlation of the current with the plasma luminosity. The chamber pressure resulting from the evolving plasma is also included in Fig. 13 to illustrate the pressure corresponding to each image in the closed chamber. As one can see, both test configurations generated plasma jets that exhibit the features of underexpanded supersonic jets. However, differences are also evident. In open air, because the ambient pressure is constant at 1 atm, the jet keeps growing after emerging from nozzle exit until it reaches a fully developed state around $t = 120$ μs, after which it varies little in its structure and size. However, in the closed chamber, because the ambient conditions (pressure and temperature) are changing with time over the event, the jet size undergoes a growing (in length and breadth) and then shrinking (in breadth) process, and the shock system is also varying, that is, the barrel shock is shrinking and Mach disk is pushed back toward nozzle exit due to the increasing pressure in the chamber. This dynamic feature suggests that the increase of chamber pressure would lead to a decrease in jet penetration through the charge bed of an ETC gun. In early times, however, for example, when $t = 60$ μs, because chamber pressure is still low, the jet grows very fast. In general, the jet has a much smaller size in a chamber than in open air under the same test conditions. Accordingly, the overall density in the plasma within the jet should be greater in the chamber than in open air and a more aggressive plasma–propellant interaction can be expected.

Figure 14 shows burning JA2 and plasma-induced high-temperature gases in the closed chamber; also included are the corresponding burning pressure trace and plasma pressure from a baseline test with an inert substitute sample. The top row in Fig. 14 shows that ignition occurred no later than 10 ms after firing the plasma, and evidence of ignition was seen at multiple spots, an indication of fragmentation of the propellant sample, which is possible given the small thickness (2.3 mm) of JA2 sample and the short nozzle–sample distance (3 mm). The test with an inert sample shown in the bottom row of Fig. 14 indicates that the brightness in images at 5 ms mostly comes from plasma-generated hot gases. Furthermore Fig. 14 shows gas motion that accompanies the burning process, resulting from expansion into the chamber. As a comparison, Fig. 15 presents a test that employed an even thinner (1.8-mm) JA2 sample to increase the likelihood of fragmentation. As can be clearly seen, from $t = 10$ ms, a fragment was captured, as was its movement with the gas.

Conclusions

Experiments have been conducted in closed chambers to study the behavior of JA2 propellant during exposure to an ETC plasma. The results from parametric studies indicated that plasma energy has a significant influence on ignition and combustion of the propellant. At low plasma energies, rapid, plasma-driven burning occurred, but self-sustained burning was not achieved. With moderate plasma energies, combustion of the propellant exhibited a two-stage burning behavior: one stage of plasma-driven rapid burning that occurred during the plasma pulse and a second stage of slower self-sustained burning, which occurred with a clear delay after the first stage. When plasma energy was increased further, the two-stage behavior became less distinct and eventually disappeared, leaving only one stage of burning. Nozzle length and diameter affected the ignition

and combustion characteristics as a result of energy losses from the plasma as it flows through the nozzle. The propellant burning behavior is also affected by both nozzle–sample distance and sample thickness.

The plasma luminosity is considerably brighter than that of burning JA2, so that it was not possible to capture the ignition and plasma-driven burning of the propellant during the pulse. Hence, the ignition delay was sufficiently prolonged through using a large test chamber to separate the ignition and burning of the propellant from the plasma pulse. Consequently, only burning images (Figs. 14 and 15) in the second stage were captured. The images revealed vigorous motion of hot gases in the closed chamber, which was induced by the plasma jet and are expected to enhance heat transfer and, thus, to enhance the burn rate. Under certain test conditions, fragments of the propellant were clearly visible in the photographs, suggesting that fragmentation occurs before and/or during the ignition and combustion processes.

Results from this experimental work should aid in the formation of a more complete understanding of plasma–propellant interaction and provide information needed to optimize the development of the plasma igniter for ETC propulsion applications.

Acknowledgments

This work was supported by the U.S. Army Research Office under Contract DAAG55-98-1-0519 with the management of David Mann. The authors are also grateful to Johnny Yu at ATK (Alliant Techsystems)–Radford Army Ammunition Plant for the shipment of the JA2 propellant.

References

[1]Fair, H. D., "Electric Launch Science and Technology in the United States," *IEEE Transactions on Magnetics*, Vol. 39, No. 1, 2003, pp. 11–17.

[2]Haugh, D. C., and Gilbert, S., "U.K. Electric Gun National Overview," *IEEE Transactions on Magnetics*, Vol. 39, No. 1, 2003, pp. 18–21.

[3]Jung, J.-W., Kim, S.-H., and Yang, K.-S., "Overview of ETC Research in Korea," *IEEE Transactions on Magnetics*, Vol. 39, No. 1, 2003, pp. 22–23.

[4]Lehmann, P., "Overview of the Electric Launch Activites at the French–German Research Institute of Saint-Louis (ISL)," *IEEE Transactions on Magnetics*, Vol. 39, No. 1, 2003, pp. 24–28.

[5]Rutberg, P. G., Shvetsov, G. A., and Savvateev, A. F., "Results of Recent Research on Electromagnetic Launch Technology in Russia," *IEEE Transactions on Magnetics*, Vol. 39, No. 1, 2003, pp. 29–35.

[6]Weise, T. H. G. G., Maag, J., Zimmermann, G., Eisenreich, N., and Derlich, H., "National Overview of the German ETC Program," *IEEE Transactions on Magnetics*, Vol. 39, No. 1, 2003, pp. 35–38.

[7]Wang, Y., Cheng, S., and Zheng, P., "Widely Developing Electric Launch Technology in China," *IEEE Transactions on Magnetics*, Vol. 39, No. 1, 2003, pp. 39–41.

[8]Katulka, G. L., and Dyvik, J. A., "Experimental Results of Electrical Plasma Ignition in 120-mm Solid Propellant Tank Gun Firings," *Proceedings of the 33rd JANNAF Combustion Meeting*, CPIA Publ. 653, Vol. 3, Chemical Propulsion Information Agency, Laurel, MD, 1996, pp. 103–110.

[9]Marinos, C., "ETC Ignition and Temperature Sensitivity," *Proceedings of the 32nd JANNAF Combustion Meeting*, CPIA Publ. 631, Vol. 3, Chemical Propulsion Information Agency, Laurel, MD, 1995, pp. 109–118.

[10]Dyvik, J. A., and Katulka, G. L., "ETC Temperature Compensation: Experimental Results of 120-mm Test Firings," *Proceedings of the 33rd JANNAF Combustion Meeting*, CPIA Publ. 653, Vol. 1, Chemical Propulsion Information Agency, Laurel, MD, 1996, pp. 111–119.

[11]Del Guercio, M., "Propellant Burn Rate Modification by Plasma Injection," *Proceedings of the 34th JANNAF Combustion Meeting*, CPIA Publ. 662, Vol. 1, Chemical Propulsion Information Agency, Laurel, MD, 1997, pp. 35–42.

[12]Chaboki, A., Zelenak, S., and Isle, B., "Recent Advances in Electrothermal–Chemical Gun Propulsion at United Defense, L. P.," *IEEE Transactions on Magnetics*, Vol. 33, No. 1, 1997, pp. 284–288.

[13]Wren, G. P., and Oberle, W. F., "Influence of High Loading Density Charge Configurations on Performance of Electrothermal–Chemical (ETC) Guns," *IEEE Transactions on Magnetics*, Vol. 37, No. 1, 2001, pp. 211–215.

[14]Perelmutter, L., Sudai, M., Goldenberg, C., Kimhe, D., Zeevi, Z., Arie, S., Melnik, M., and Melnik, D., "Plasma Propagation and Ignition in the Chamber of a SPETC Gun," *IEEE Transactions on Magnetics*, Vol. 35, No. 1, 1999, pp. 213–217.

[15]Del Guercio, M., Stobie, I., Katulka, G., and Oberle, W., "A Pulse Forming Network Design for Electrothermal–Chemical Combustion Characterization of Solid Propellants," *Tenth IEEE International Pulsed Power Conference, Digest of Technical Papers*, Vol. 1, Inst. of Electrical and Electronics Engineers, New York, 1995, pp. 279–285.

[16]Koleczko, A., Ehrhardt, W., Kelzenberg, S., and Eisenreich, N., "Plasma Ignition and Combustion," *Propellants, Explosives, Pyrotechnics*, Vol. 26, 2001, pp. 75–83.

[17]Birk, A., Del Guercio, M., Kinkennon, A., Kooker, D. E., and Kaste, P., "Interrupted-Burning Tests of Plasma-Ignited JA2 and M30 Grains in a Closed Chamber," *Propellants, Explosives, Pyrotechnics*, Vol. 25, 2000, pp. 133–142.

[18]Beyer, R. A., "Small Scale Experiments in Plasma Propellant Interactions," *Proceedings of 37th JANNAF Combustion Subcommittee Meeting*, CPIA Publ. 701, Vol. 1, 2000, pp. 137–144.

[19]Kohel, J. M., Su, L. K., Clemens, N. T., and Varghese, P. L., "Emission Spectroscopic Measurements and Analysis of a Pulsed Plasma Jet," *IEEE Transactions on Magnetics*, Vol. 35, No. 1, 1999, pp. 201–206.

[20]Li, J. Q., Zhou, H., Kudva, G., Thynell, S., and Litzinger, T., "Experimental Investigation of Plasma Propellant Interactions," *Proceedings of 37th JANNAF Combustion Subcommittee Meeting*, CPIA Publ. 701, Vol. 1, Chemical Propulsion Information Agency, Laurel, MD, 2000, pp. 109–121.

[21]Edwards, C. M., Bourham, M. A., and Gilligan, J. G., "Experimental Studies of the Plasma-Propellant Interface for Electrothermal-Chemical Launchers," *IEEE Transactions on Magnetics*, Vol. 35, No. 1, 1999, pp. 404–409.

[22]Taylor, M. J., "Formation of Plasma Around Wire Fragments Created by Electrically Exploded Copper Wire," *Journal of Physics D: Applied Physics*, Vol. 35, No. 7, 2002, pp. 700–709.

[23]Katulka, G. L., "Parametric Study of High Energy Plasmas for Electrothermal–Chemical Propulsion Applications," *IEEE Transactions on Plasma Science*, Vol. 25, No. 1, 1997, pp. 66–72.

[24]Nusca, M. J., McQuaid, M. J., and Anderson, W. R., "Numerical Model of the Plasma Jet Generated by an Electrothermal–Chemical Igniter," *Journal of Thermophysics and Heat Transfer*, Vol. 16, No. 1, 2002, pp. 157–160.

[25]Kim, J. U., Clemens, N. T., and Varghese, P. L., "Experimental Study of the Transient Underexpanded Jet Generated by Electrothermal Capillary Plasma," *Journal of Propulsion and Power*, Vol. 18, No. 6, 2002, pp. 1153–1160.

[26]Li, J. Q., Kwon, J., Thynell, S. T., and Litzinger, T. A., "Experimental Investigations of Characteristics of Electro–Thermal–Chemical Plasma," AIAA Paper 2001-3855, July 2001.

[27]White, K. J., Katulka, G. L., Khuan, T., and Nekula, K., "Plasma Characterization for Electrothermal–Chemical (ETC) Gun Applications," U.S. Army Research Lab., Rept. ARL-TR-1491, Aberdeen Proving Grounds, MD, 1997.

[28]Powell, J. D., and Zielinski, A. E., "Capillary Discharge in the Electrothermal Gun," *IEEE Transactions on Magnetics*. Vol. 29, No. 1, 1993, pp. 591–596.

[29]Taylor, M. J., and Dunnett, J., "A Description of the Wire Explosion Process for the ETC Plasma Generators," *IEEE Transactions on Magnetics*, Vol. 39, No. 1, 2003, pp. 269–274.

[30]Perelmutter, L., Sudai, M., Goldenberg, C., Kimhe, D., Zeevi, Z., Arie, S., Melnik, M., and Melnik, D., "Plasma Propagation and Ignition in the Chamber of a SPETC Gun," *IEEE Transactions on Magnetics*, Vol. 35, No. 1, 1999, pp. 213–217.

[31]Pesce-Rodriguez, R. A., Beyer, R. A., Kinkennon, A. E., Del Guercio, M., Kaste, P. J., and Newberry, J. E., "In-depth Chemistry in Plasma-Exposed M30 and JA2 Gun Propellants," *Proceedings of the 37th JANNAF Combustion Subcommittee Meeting*, CPIA Publ. 701, Vol. 1, Chemical Propulsion Information Agency, Columbia, MD, 2000, pp. 145–155.

[32]Beyer, R. A., and Pesce-Rodriguez, R. A., "Experiments to Define Plasma–Propellant Interactions," *IEEE Transactions on Magnetics*, Vol. 39, No. 1, 2003, pp. 207–211.

[33]Katulka, G. L., White, K. J., Oberle, W. F., Kaste, P. J., Pesce-Rodriguez, R. A., and Leadore M. L, "Experimental Characterization of Plasma Effects on Energetic Materials for Electrothermal–Chemical Launch Applications," *IEEE Transactions on Magnetics*, Vol. 35, No. 1, 1999, pp. 197–200.

[34]Bourham, M. A., Gilligan, J. G., and Oberle, W. F., "Analysis of Solid Propellant Combustion Behavior Under Electrothermal Plasma Injection for ETC Launchers," *IEEE Transactions on Magnetics*, Vol. 33, No. 1, 1997, pp. 278–283.

[35]Taylor, M. J., "Evidence for the Hypothesis of Ignition of Propellants by Metallic Vapour Deposition," *Propellants, Explosives, Pyrotechnics*, Vol. 27, 2002, pp. 327–335.

[36]Taylor, M. J., "Consideration of the Energy Transfer Mechanisms Involved in SPETC Ignition Systems,"*IEEE Transactions on Magnetics*, Vol. 39, No. 1, 2003, pp. 262–268.

[37]Li, J. Q., Litzinger, T. A., and Thynell, S. T., "Experimental Investigation of Plasma-Ignition and Combustion of Solid Propellants," *Proceedings of the 39th JANNAF Combustion Subcommittee Meeting*, CPIA Publ. 780, Vol. 3, Chemical Propulsion Information Agency, Laurel, MD, 2003.

[38]Kappen, K., and Beyer, R. A., "Progress in Understanding Plasma–Propellant Interaction," *Propellants, Explosives, Pyrotechnics*, Vol. 28, No. 1, 2003, pp. 32–36.

[39]Li, J. Q., Litzinger, T. A., and Thynell, S. T., "Interaction of Capillary Plasma with Double-Base and Composite Propellants," *Journal of Propulsion and Power*, Vol. 20, No. 4, 2004, pp. 675–683.

[40]Kim, B. G., Yu, M. S., Cho, Y., and Cho, H. H., "Distributions of Recovery Temperature on Flat Plate by Underexpanded Supersonic Impinging Jet," *Journal of Thermophysics and Heat Transfer*, Vol. 16, No. 3, 2002, pp. 425–431.

[41]Lamont, P. J., and Hunt, B. L., "The Impingement of Underexpanded, Axisymmetric Jets on Perpendicular and Inclined Flat Plates," *Journal of Fluid Mechanics*, Vol. 100, Pt. 3, 1980, pp. 471–511.

[42]Williams, A. W., and White, K. J., "Plasma–Propellant Interactions Studies: Measurements of Heat Flux Produced by Hydrocarbon Ablation-Supported Plasmas," *IEEE Transactions on Magnetics*, Vol. 37, No. 1, 2001, pp. 203–206.